Heliyon 6 (2020) e03517

Contents lists available at ScienceDirect

Heliyon

journal homepage: www.cell.com/heliyon

Research article

Design and *in silico* screening of aryl allyl mercaptan analogs as potential histone deacetylases (HDAC) inhibitors

Sugandha Singhal [a], Mallika Pathak [b], Paban K. Agrawala [c], Himanshu Ojha [d,*]

[a] *Synthetic Organic and Natural Products Laboratory, University School of Basic and Applied Sciences, Guru Gobind Singh Indraprastha University, Sector 16-C, Dwarka, New Delhi, 110078, India*
[b] *Department of Chemistry, Miranda House, University of Delhi, Delhi, 110007, India*
[c] *Department of Radiation Genetics and Epigenetics,Division of Radiation Biodosimetry, Institute of Nuclear Medicine & Allied Sciences, Delhi, 110054, India*
[d] *CBRN Protection and Decontamination Research Group, Division of CBRN Defence, Institute of Nuclear Medicine and Allied Sciences (INMAS) DRDO, Delhi, 110054, India*

ARTICLE INFO

Keywords:
Pharmaceutical chemistry
Theoretical chemistry
Histone deacetylase
Allylmercaptan
DFT
Pharmacotoxicity
Docking

ABSTRACT

The Zn^{+2} HDACIs show promising anticancer activity. Allyl mercaptan (AM), a metastabilzed monomeric form of diallyl disulphide (DADS) shows better HDACI activity. The present work screens a dataset of aryl AM derivatives **1(a-g)** for potential HDACI action *via in silico* models. DFT calculations predicted the geometrical parameters and frontier orbital calculations suggested better chemical reactivity. Negative chemical potential and NBO hyper conjugative interactions predicted their chemical stability. ADME study confirmed favourable drug likeliness. Molecular docked models suggested the formation of coordinate bond between sulphur of allylmercaptan and Zn^{2+} cofactor of HDAC8. Besides, models also predicted the dominance of hydrophobic interactions. The aryl AM analogs docked perfectly with HDAC3 as well. The glide score and S-Zn distance of compounds **1a, 1f and 1g** were found to be better than allylmercaptan. Therefore, the designed aryl AM analogs filtered as better HDACIs. These could be further used for design and synthesis of new improved HDACIs.

1. Introduction

HDAC inhibitors have gained the interest of researchers possibly due to their potency and diverse pharmacological applications. Various structurally diverse HDAC inhibitors possess anti-tumor, anti-histaminic, anti-inflammatory and immune modulatory properties. HDACIs have been known to inhibit induction and proliferation, induce differentiation, and influence a variety of processes such as cell cycle arrest, angiogenesis, and apoptosis of tumor cells in culture and in animal models [1, 2].

The Zn^{2+} dependent HDACIs have been widely studied as anticancer drugs to suppress the general action of catalyzing deacetylase activity of HDACs in presence of Zn^{2+} as essential cofactor. Among the four classes of HDACs classes I, II, and IV are inhibited by Zn^{2+} binding HDACIs. However, class III HDACs is structurally homologous with the yeast Sir2 protein and requires NAD^{+} as a cofactor instead of Zn^{2+} [3, 4]. In class I, HDACs 1, 2, 3 and 8 are mostly preferred for binding studies as they are localized in the nucleus, most abundant and ubiquitously-expressed [5]. The wide active pocket and a larger surface area of HDAC8 is an interesting feature which distinguishes it from other HDAC enzymes [6]. HDAC8 is ubiquitously expressed in all human tissues and organs as reported in experiments performed on total tissue extracts [7, 8, 9]. Thus HDAC8 is the most acceptable receptor for such HDAC inhibition. HDAC3 has a unique recruitment to SMRT complex where it interacts with conserved DAD [10, 11, 12, 13, 14, 15]. The Ser424 residue in the active site of HDAC3 is primarily phosphorylated. Thus dephosphorylation of Ser424 on HDAC3 inhibits HDAC3 activity possibly due to a conformational change that renders it less active. The three FDA approved HDACIs, vorinostat, belinostat and romidepsin have shown considerable anti-cancer activity [16, 17, 18].

The dietary compounds such as sulforane, genistein, tea polyphenol-catechins, curcumin, diallyl disulphide and revestrol play an important role in regulating key molecular targets like HDAC, DNA methyl-transferases etc for the treatment of various diseases [19, 20]. Diallyldisulphide (DADS) a dietary organosulphur compound exhibits excellent HDAC inhibitory activity, anti-microbial, anti-inflammatory, anticancer, anti-oxidant and antihistaminic activity [21, 22, 23, 24].

* Corresponding author.
E-mail address: Himanshu.drdo@gmail.com (H. Ojha).

https://doi.org/10.1016/j.heliyon.2020.e03517
Received 2 November 2019; Received in revised form 30 January 2020; Accepted 27 February 2020

Table 1. Aryl allyl mercaptan derivatives with electron withdrawing substituents.

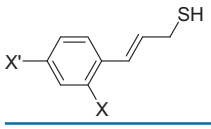

Compound no.	X	X′
1a	H	NO_2
1b	Cl	H
1c	Cl	Cl
1d	Br	H
1e	Br	Br
1f	H	F
1g	H	CF_3

Table 2. Designed aryl allyl mercaptan compounds with electron withdrawing substituents.

Property	Compounds							
	1a	1b	1c	1d	1e	1f	1g	AM
Log P	2.94	3.44	4.09	3.57	4.35	3.15	3.59	1.28
TPSA	45.82	38.80	38.80	38.80	38.80	38.80	38.80	38.80
Natoms	13	11	12	11	12	11	14	4
MW	195.24	184.69	219.13	215.11	308.03	168.23	218.24	74.15
nOH	3	0	0	0	0	0	0	0
nOHNH	0	0	0	0	0	0	0	0
Nviolations	0	0	0	0	0	0	0	0
Nrotb	3	2	2	2	2	2	3	1
Volume	169.26	159.46	172.99	163.81	181.69	150.85	174.38	74.83

Table 3. Designed aryl allyl mercaptan compounds with electron withdrawing substituents.

Property	Compounds							
	1a	1b	1c	1d	1e	1f	1g	AM
BBB	1.96	1.36	1.02	1.30	0.98	1.65	1.19	1.19
Caco2	18.56	58.14	58.48	57.75	58.51	55.51	54.24	54.78
HIA	84.18	98.11	98.05	98.03	98.27	98.46	98.36	96.86
MDCK	35.75	42.13	11.28	0.14	0.18	132.15	36.60	137.61
PPB	83.66	73.28	90.85	78.18	91.69	75.74	87.65	50.56
SP	-2.21	-1.02	-0.99	-0.93	-0.80	-1.20	-0.77	-1.93

BBB: Blood Brain Barrier, HIA: Human Intestinal Absorption, PPB: Plasma Protein Binding, SP: Skin Permeability.

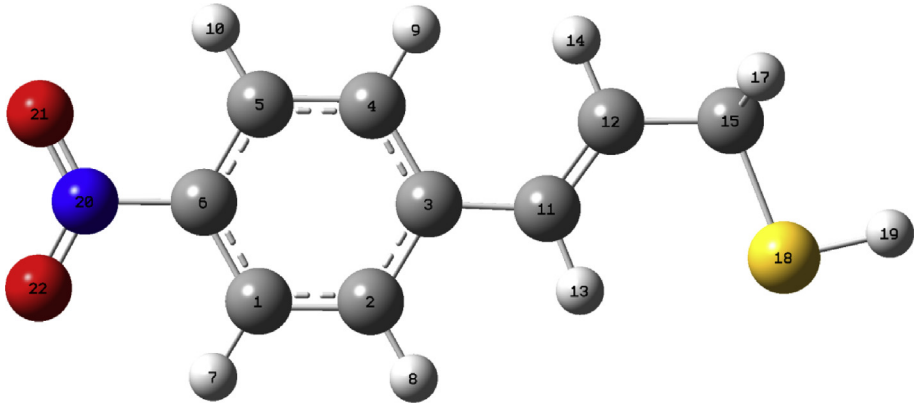

Figure 1. Ground state optimized structure of aryl AM **1a** at B3LYP/6-311G++(d,p) level.

Table 4. Theoretical optimized geometrical properties of aryl AM **1a** at B3LYP/6-311G++(d,p) level.

Bond length (Å)	Theoretical calculated	Bond angle ()	Theoretical calculated	Bond dihedral ()	Theoretical calculated
C1-C2	1.387				
C2-C3	1.399	C1-C2-C3	120.44		
C3-C4	1.398	C2-C3-C4	119.19	C1-C2-C3-C4	-0.05
C4-C5	1.386	C3-C4-C5	120.71	C2-C3-C4-C5	0.04
C5-C6	1.400	C4-C5-C6	119.86	C3-C4-C5-C6	0.03
H7-C1	1.099	H7-C1-C2	119.31	H7-C1-C2-C3	179.96
H8-C2	1.096	H8-C2-C1	119.61	H8-C2-C1-C6	-179.93
H9-C4	1.102	H9-C4-C3	118.65	H9-C4-C3-C2	-179.82
H10-C5	1.099	H10-C5-C4	119.38	H10-C5-C4-C3	-179.94
C11-C3	1.459	C11-C3-C2	119.61	C11-C3-C2-C1	179.98
C12-C11	1.339	C12-C11-C3	122.41	C12-C11-C3-C2	-179.07
H13-C11	1.098	H13-C11-C3	116.34	H13-C11-C3-C2	0.95
H14-C12	1.104	H14-C12-C11	120.08	H14-C12-C11-C3	-0.58
C15-C12	1.479	C15-C12-C11	122.99	C15-C12-C11-C3	179.14
H16-C15	1.105	H16-C15-C12	111.93	H16-C15-C12-C11	5.79
H17-C15	1.106	H17-C15-C12	108.90	H17-C15-C12-C11	-111.29
S18-C15	1.827	S18-C15-C12	108.06	S18-C15-C12-C11	128.09
S18-H19	1.307	H19-S18-C15	99.02	H19-S18-C15-C12	174.53
N20-C6	1.495	N20-C6-C5	120.15	N20-C6-C5-C4	179.92
O21-N20	1.215	O21-N20-C6	119.48	O21-N20-C6-C5	-0.78
O22-N20	1.215	O22-N20-C6	119.48	O22-N20-C6-C5	179.29

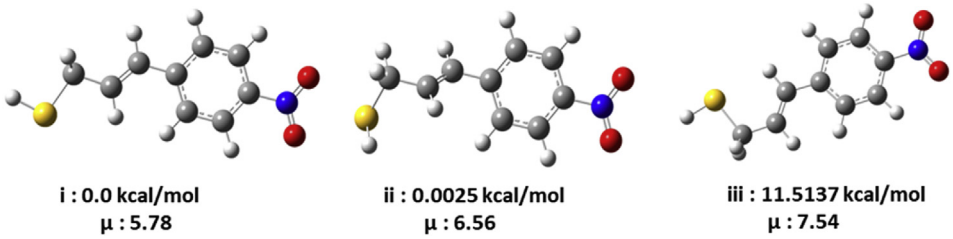

Figure 2. Optimized ground state geometries of conformers of aryl AM **1a** at B3LYP/6-311G++(d,p) level with their relative Gibbs free energies.

Table 5. Representative Relative Gibbs free energies of **1(b-g)** conformers indicating the most stable conformation.

CONFORMERS	RELATIVE GIBBS FREE ENERGIES (HARTREES)					
	1b	1c	1d	1e	1f	1g
1	0	0	0	0	0	0
2	0.0002	18.7145	2.7603	0.0001	0.0001	0.0005
3	0.0003	18.7154	2.7614	0.0002	0.0002	0.0009
4	0.0034	18.7155	2.7615	0.0010	0.0002	0.0027
5	0.0035	18.7180	36.9312	0.0011	0.0009	0.3430
6	0.0048	18.7181	36.9374	0.0014	0.0026	4.0966

DADS has been reported to metabolize to allylmercaptan (AM) within 30 min of administration. The inhibitory HDAC action of AM was reported better compared to its precursors Diallyldisulfide (DADS) and S-allylmercaptocysteine (SAMC) under cell-free conditions [25, 26, 27]. Compounds containing thiol moiety such as allyl alcohol and mercaptoethanol have been found to abolish and decrease HDAC inhibitory activity respectively in contrast to compounds containing sulfhydryl group. Therefore the sulfhydryl group of AM plays a major role in HDAC inhibition. Various compounds prepared using synthetic strategies with -$(CH)_2$-SH group have been reported with strong HDAC inhibitory action majorly due to -S-Zn binding within the active site [28, 29].

Owing to the fact that diallyl disulphide metabolizes to AM within few minutes of administration, in the present study the allyl mercaptan moiety of the pre-synthesized DADS derivatives by *Rai et al.* [30] have been screened for their pharmacokinetics, drug likeliness and potential HDAC inhibitory action *via in silico* DFT, ADME and molecular docking studies.

2. Methodology

A preliminary dataset of 7 aryl AM derivatives (Table1) was selected with electron withdrawing substituents. The derivatives were screened for their drug likeliness and non-toxicity *via in silico* studies. The most reactive positions in these compounds were screened using DFT (Frontier orbital and NBO) calculations. The compounds were further screened for their potential HDAC inhibitory activity *via* Molecular docking study.

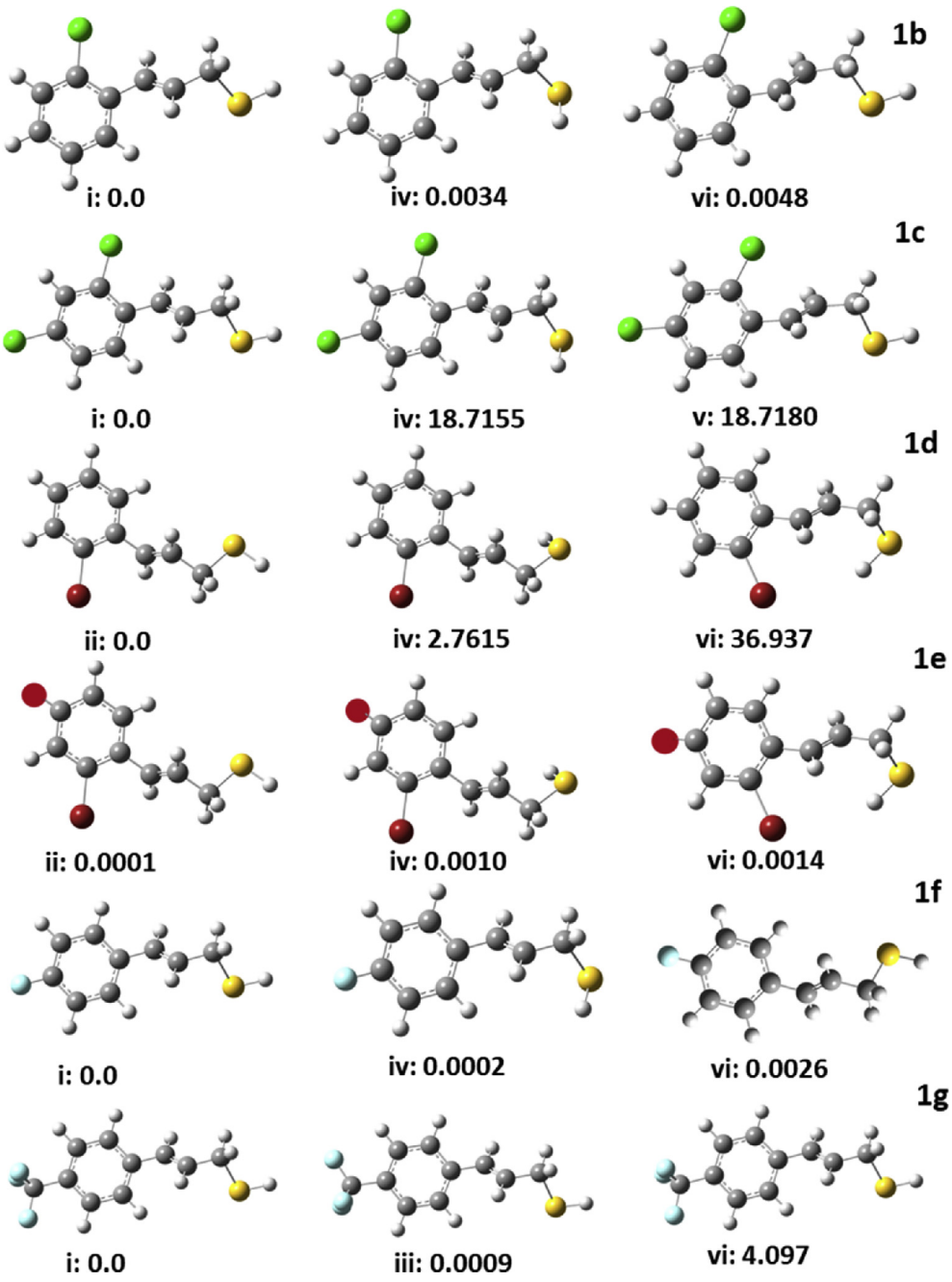

Figure 3. Optimized ground state geometries of most stable conformers of i)**1b**, ii) **1c**, iii) **1d**, iv) **1e**, v) **1f** and vi) **1g** at B3LYP/6-311G++(d,p) level with their relative gibbs free energies (kcal/mol).

Table 6. The electronic properties of compounds calculated at DFT-B3LYP/6-311G++(d,p) level.

Compound	E_{HOMO}(KJ/mol)	E_{LUMO}(KJ/mol)	E_L–E_H (KJ/mol)	η(KJ/mol)	μ(KJ/mol)
1a	-0.1283	0.0167	0.145	0.0725	-0.1116
1b	-0.2452	0.2071	0.452	0.4523	-0.0381
1c	-0.2515	0.1901	0.441	0.4416	-0.0614
1d	-0.1211	0.0487	0.169	0.1698	-0.0724
1e	-0.1278	0.0513	0.171	0.1734	-0.0803
1f	-0.1165	0.0599	0.176	0.1764	-0.0566
1g	-0.1216	0.0486	0.170	0.1702	-0.0730
AM	-0.2642	0.0276	0.236	0.1459	-0.1183

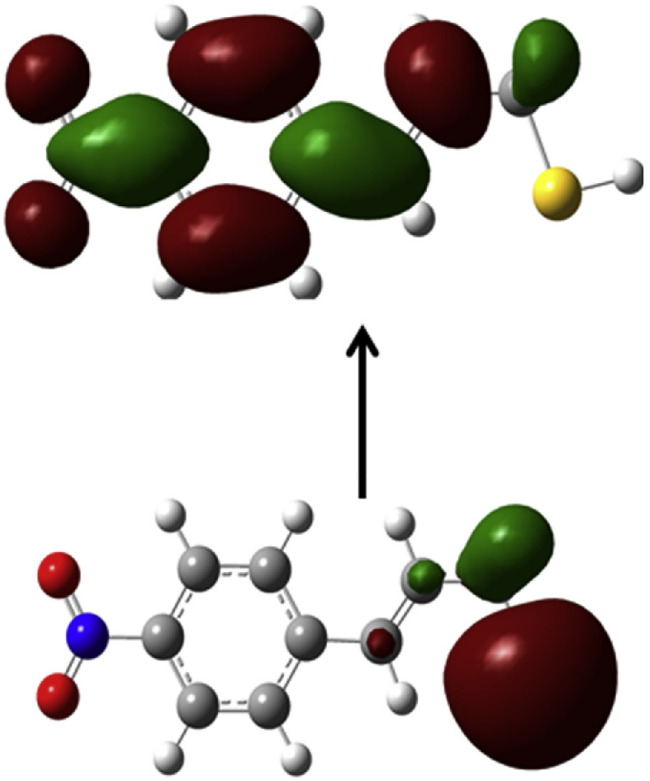

Figure 4. Frontier orbital diagram of **1a** using DFT-B3LYP/6-311G++(d,p) method with frontier orbital gap value of 0.145 kcal/mol.

2.1. Calculation of druglikeliness properties

The molecular properties of compounds **1a-g** were calculated using the Molinspiration cheminformatics software (www.molinspiration.com). The major druglikeliness parameters calculated include number of atoms, molecular weight, partition coefficient (LogP), hydrogen bond acceptors and donors, topological surface area (TPSA), and Lipinski's rule violations [31].

2.2. Pharmacokinetic and toxicity parameters

PreADMET online server 2.0 version [32]was used to calculate adsorption, distribution, metabolism and excretion (ADME) parameters. The properties calculated were plasma protein binding (PPB), human intestinal absorption (HIA), logKp (degree of skin permeation), Caco2 cell lines and MDCK cell lines barrier penetration. These predicted the oral absorption of the compounds [33].

2.3. Geometry optimization using density functional theory (DFT)

DFT study illustrates the electronic structural properties of the molecules. The DFT calculations were done using Gauss View 5.0 [34] molecular visualization program and Gaussian 09 program [35]. The molecular structures of the aryl AM compounds in the ground state were optimized at B3LYP/6-311G++(d,p) level of computation [36].

The optimized ground state geometry of the most stable conformer was used to predict different structural parameters like bond lengths, bond angles, and dihedral angles.

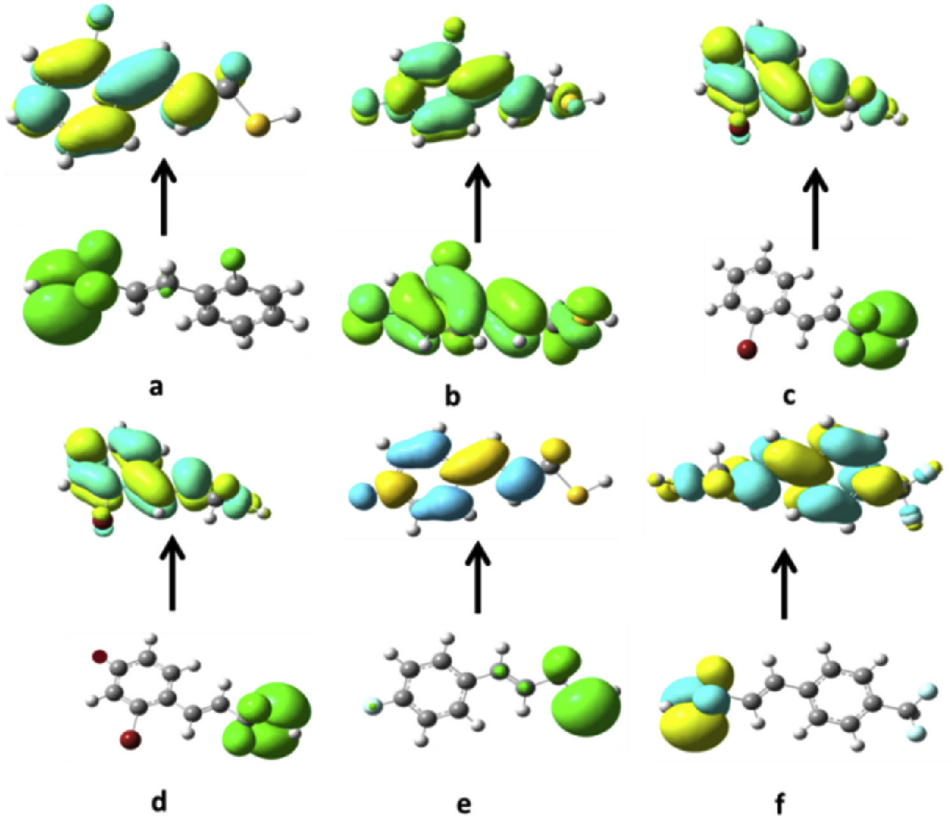

Figure 5. Frontier orbital diagram **a)1b** with frontier orbital gap of 0.452, **b) 1c** with frontier orbital gap value of 0.441, **c) 1d** with frontier orbital gap of 0.169, **d)1e** with frontier orbital gap of 0.171, **e) 1f** with frontier orbital gap of 0.176, **f) 1g** with frontier orbital gap of 0.170.

Table 7. Second order perturbation analysis of the interaction between donor and acceptor orbitals of compound **1a** calculated B3LYP/6–311++G(d,p).

Donor (i)	Type	ED/e	Acceptor(j)	Type	ED/e	E(2)[a]	E(j)-E(i)[b]	F(i,j)[c]
C1-C2	σ	1.983	C6-N20	σ*	0.153	2.79	0.84	0.045
C1-C2	σ	1.676	C3-C4	π *	0.365	20.32	0.28	0.068
C1-C2	σ	1.676	C5-C6	π*	0.378	21.63	0.27	0.070
C1-C6	σ	1.982	C6-N20	σ*	0.153	2.65	0.85	0.044
C1-H7	σ	1.983	C2-C3	σ*	0.017	2.11	1.03	0.042
C1-H7	σ	1.983	C5-C6	σ*	0.019	2.02	1.04	0.041
C2-H8	σ	1.985	C1-C6	σ*	0.019	2.18	1.04	0.043
C3-C4	σ	1.608	C1-C2	π*	0.314	20.51	0.27	0.068
C3-C4	σ	1.608	C5-C6	π *	0.378	25.00	0.26	0.073
C3-C4	σ	1.608	C11-C12	π *	0.083	10.87	0.30	0.056
C3-C11	σ	1.977	C12-C15	σ*	0.018	2.36	0.96	0.042
C4-C5	σ	1.982	C6-N20	σ*	0.153	2. 76	0.84	0.044
C4-H9	σ	1.984	C5-C6	σ*	0.019	2.22	1.04	0.043
C5-C6	σ	1.982	C6-N20	σ*	0.153	2.66	0.85	0.044
C5-C6	σ	1.652	C1-C2	π*	0.315	21.67	0.29	0.071
C5-C6	σ	1.652	C3-C4	π*	0.365	20.41	0.29	0.069
C5-C6	σ	1.652	N20-O22	σ*	0.680	13.50	0.17	0.046
C5-H10	σ	1.983	C1-C6	σ*	0.019	2.02	1.04	0.041
C5-H10	σ	1.983	C3-C4	σ*	0.018	2.13	1.03	0.042
C6-N20	σ	1.964	N20-O21	σ*	0.069	5.89	0.97	0.068
C6-N20	σ	1.964	N20-O22	σ*	0.069	5.89	0.97	0.068
C11-C12	σ	1.919	C3-C4	π *	0.018	11.68	0.30	0.057
C11-C12	σ	1.919	C15 -S18	σ*	0.015	2.88	0.49	0.034
C11-H13	σ	1.983	C12-H14	σ*	0.017	3.21	0.93	0.049
C12-H14	σ	1.984	C11-H13	σ*	0.015	2.96	0.94	0.047
C12-C15	σ	1.983	S 18	RY*(1)	0.003	0.68	1.12	0.025
C12-C15	σ	1.983	C3-C11	σ*	0.025	2.86	0.97	0.047
C15-H16	σ	1.992	S 18	RY*(2)	0.002	0.53	1.08	0.021
C15-H17	σ	1.983	C11-C12	σ*	0.084	2.66	0.57	0.035
C15-S18	σ	1.973	C11-C12	σ*	0.084	4.55	0.53	0.044
S18-H19	σ	1.992	C12-C15	σ*	0.018	1.41	0.85	0.031
N20 -O21	σ	1.979	C6-N20	σ*	0.153	3.60	0.97	0.054
N20 -O21	σ	1.979	N20-O22	σ*	0.069	6.12	1.07	0.073
N20 -O22	σ	1.979	C6-N20	σ*	0.153	3.60	0.97	0.054
N20-O22	σ	1.979	N20-O21	σ*	0.069	6.12	1.07	0.073
N20-O22	σ	1.983	O 21	LP (3)	1.356	13.43	0.19	0.078
N20-O22	σ	1.983	C5-C6	σ*	0.379	5.15	0.38	0.044
N20-O22	σ	1.983	N20-O22	σ*	0.680	10.46	0.27	0.058
S 18	CR (3)	2.000	S 18	RY*(3)	0.000	0.52	6.30	0.051
S 18	LP (2)	1.981	C15-H16	σ*	0.017	3.58	0.56	0.040
S 18	LP (2)	1.981	C15-H17	σ*	0.014	2.16	0.56	0.031
O 21	LP (2)	1.901	C6 -N20	σ*	0.153	14.39	0.39	0.068
O 21	LP (2)	1.901	N20-O22	σ*	0.069	15.94	0.49	0.080
O 21	LP (3)	1.356	N20-O22	σ*	0.680	197.72	0.08	0.114
O 22	LP (2)	1.901	C6-N20	σ*	0.153	14.40	0.39	0.068
O 22	LP (2)	1.901	N20-O21	σ*	0.069	15.94	0.49	0.080
C3-C4	π*	0.365	C11-C12	π *	0.084	38.85	0.03	0.064
C 6-N 20	π*	0.153	N20-O21	π*	0.069	2.04	0.10	0.039
C 6-N 20	π*	0.153	N20-O22	π*	0.069	2.04	0.10	0.039
N20-O22	π*	0.680	C5-C6	π*	0.379	13.49	0.11	0.048

[a] E(2) indicates second order perturbation energy (Stabilization energy in Kcal/mol).
[b] Energy difference between donor and acceptor I and j NBO orbitals in a.u.
[c] f(I,j) is the Fock matrix elements between I and j NBO orbitals in a.u.

2.4. Frontier molecular orbital calculations

The electronic properties like frontier molecular orbital, HOMO (highest occupied molecular orbital) and LUMO (lowest unoccupied molecular orbital) energies are important for defining reactivity of a chemical species [37]. The global reactivity descriptors, chemical potential (μ) and hardness (η) described by Parr and Pearson were calculated using equations [38]:

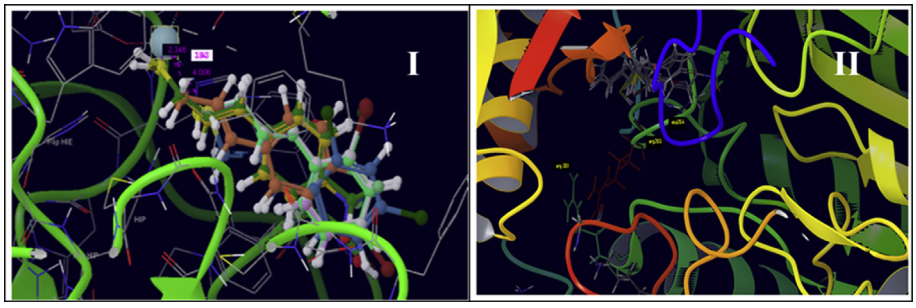

Figure 6. Binding interaction of the aryl AM designed compounds **1(a-g)** and AM (reference) with I) HDAC8 protein (PDB ID: 1T67) and II) HDAC3 protein (PDB ID: 4A69).

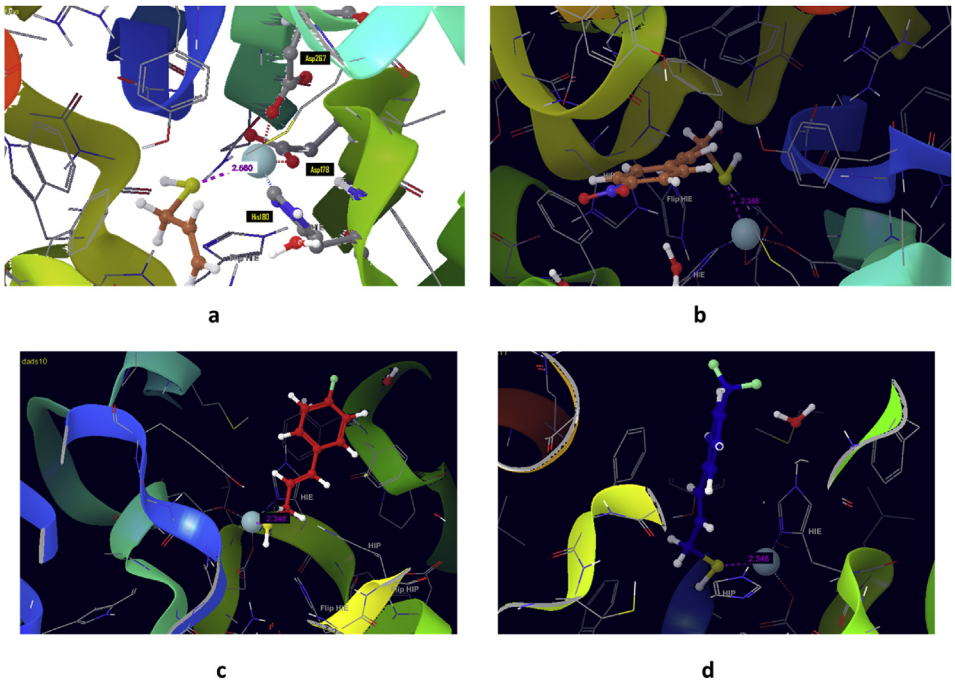

Figure 7. 3D docked models for a) allylmercaptan, b) compound **1a**, c) compound **1f** and d) compound **1g** with HDAC8 in the catalytic core with conserved interacting amino acid residues stabilizing the binding interactions.

Table 8. S-Zn bond distance and Glide score values of aryl AM compounds **1(a-g)** and AM with HDAC8 and HDAC3.

Compounds	HDAC8			HDAC3	
	Bond length (S- Zn) Å	Glide Score (Kcal/mol)	Gibbs free energy (kJ/mol)	GlideScore (Kcal/mol)	Gibbs free energy (kJ/mol)
1a	2.348	- 4.636	-29.05	-4.377	-15.41
1b	12.09	- 4.257	-20.44	-4.968	-19.06
1c	12.35	- 3.655	-19.39	-5.300	-12.77
1d	11.91	- 4.112	-20.36	-5.072	-18.21
1e	11.40	- 3.803	-21.14	-5.452	-18.33
1f	2.358	- 4.959	-30.08	-4.430	-12.66
1g	2.362	- 4.732	-29.56	-4.385	-17.73
AM (Reference)	2.56	-2.342	-25.43	-1.959	-15.61

$$\mu = -\frac{I + A}{2} \quad (1)$$

$$n = (I - A)/2 \text{ respectively} \quad (2)$$

where I is the ionization potential ($-E_{HOMO}$) and A is the electron affinity ($-E_{LUMO}$) as correlated using the Koopman's theorem [39, 40].

2.5. Natural bond order analysis (NBO)

Reed and Weinhold performed the natural bond orbital (NBO) calculations [41] which depict the second order interactions between the filled Lewis orbital to empty non-Lewis orbital of a sub-system. These interactions determine the intermolecular delocalization or hyperconjugation within a system. Considering the title compound the second

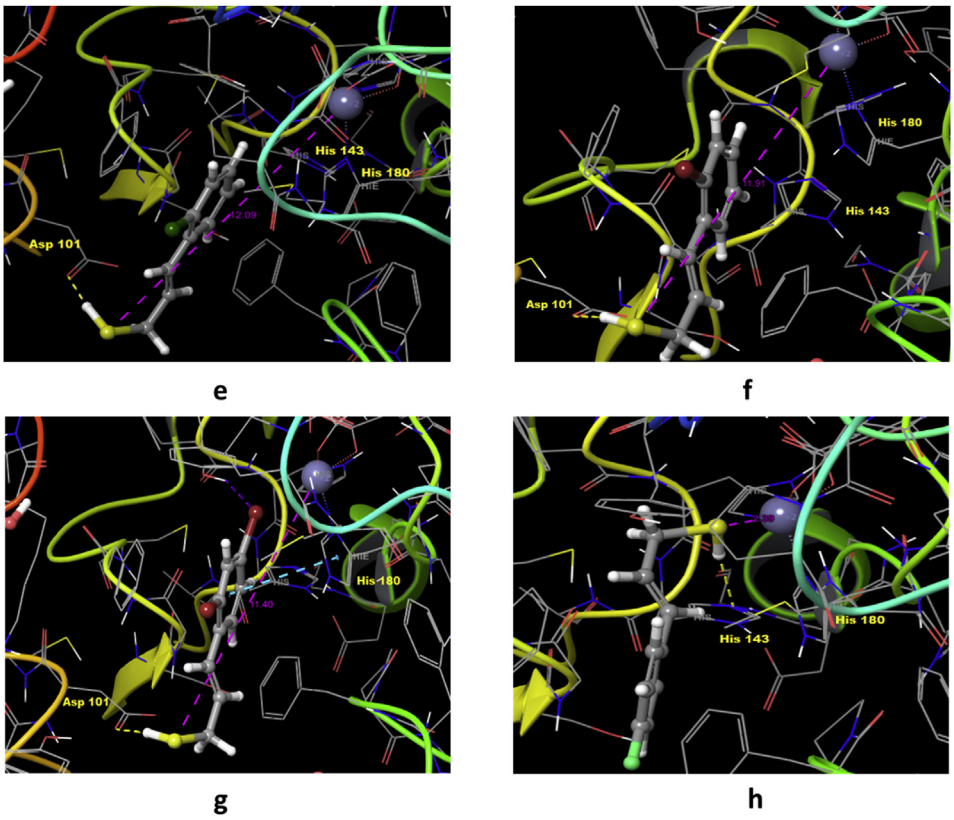

Figure 8. 3D docked models for e) compound **1b,** f) compound **1c**, g) compound **1d**, h) compound **1e**, docked in HDAC8 catalytic core with conserved interacting amino acid residues stabilizing the binding interactions.

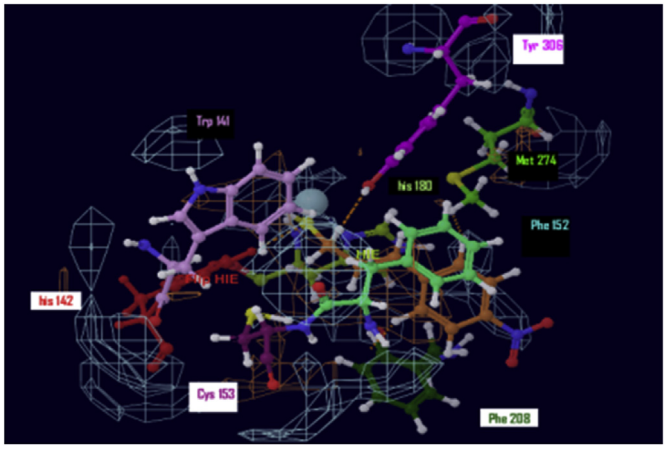

Figure 9. The dominance of hydrophobic interactions in binding of AM moieties of DADS compounds and HDAC8. The compounds **1a**, **1f** and **1g** also have good glide score values -4.63, -4.95 and -4.73 kJ/mol compared to AM (-2.34 kJ/mol, 2.56 Å).

order perturbation theory analysis for Fock matrix in NBO was carried out to evaluate donor acceptor interactions. They result in a loss of occupancy from localized NBO of Lewis structure to empty non-Lewis orbital [33]. The stabilization energy E(2), for each donor (i) and acceptor (j) is given by the formula:

$$E^{(2)} = \Delta E_{ij} = (q_i \times F(i,j)^2)/(\varepsilon_j - \varepsilon_i)$$

where q_i is the donor orbital occupancy, ε_i and ε_j are diagonal elements and F(i,j) is the off diagonal NBO Fock matrix element. These calculations allow us to analyse the probable charge-transfers and the intermolecular bond paths.

2.6. Molecular docking

The three dimensional target receptor HDAC8 (PDB ID: 1T67) and HDAC3 (PDB ID: 4A69) structures were retrieved from the Protein Data Bank (www.rcsb.org). The Schrodinger suite was used to refine protein structure via protein preparation wizard. Prime (Prime v2.0,2012) was used to add missing side chains and hydrogens to the raw protein structure. The crystallized water molecules in the active site present beyond 5 Å were removed using an all atom force field. In order to remove potential steric clashes minimizations on the protein structure were done until the RMSD value (root mean square deviation) reached 0.3 Å for non-hydrogen atoms using OPLS_2005 force field.

The lead targets were prepared using Ligprep function of the Schrödinger suite in which the energy minimization was performed using OPLS_2005 force field. A grid was generated around the receptor using Grid generation program and Glide Docking program respectively. The XP (Xtra Precision) mode of docking was selected in the present case [42, 43].

3. Results and discussion

3.1. Druglikeliness properties

The compounds **1a-g** obeyed the Lipinski's rule of five (i.e MW $<$ 500, Log P $<$ 5, number of H bond donors up to 5 and H bond acceptors up to 10) [31](Table 2). Thus these designed derivatives depicted drug like properties.

3.2. ADME parameters

The ADME parameters for the compounds **1a-g** have been given in Table 3. The human intestinal (HIA) values indicate good oral absorption as the values were above 90%. The negative Kp values indicate poor skin permeation which results in good oral absorption. The PPB values except **1e** were less than 90%. The Caco 2 values were within range of 4–70, indicative of moderate permeability. MDCK values were greater than 25 except for compounds **1c-1e**, indicative of good absorption. Apart from these factors various other parameters need to be considered. The BBB values are less than two which indicates non-neurotoxicity of these compounds. Thus these screened compounds depicted good pharmacokinetics and bioavailability.

3.3. Geometry optimization

The ground state optimized geometry of aryl AM **1a** with NH_2 substituentis is given in Figure 1. The structural parameters like bond lengths, bond angles and dihedral angles for the title molecule are given in Table 4.

The C-C bond lengths of the phenyl ring and allyl moiety are shorter than other C-C bonds verifying the double bond character of the ring and allyl C-C bonds. The average C-C bond length is 1.39 Å which is almost identical to that of diamond, and the C-H distances lie in the range 1.096–1.106 Å. The S-H bond length in aryl AM **1a** is calculated to be 1.307 Å. The preferred bond angle value between successive carbon chain bonds in phenyl ring system is around 119°. Also, the dihedral angles should be nearly 0° or 180° conferring the planarity of the compound. The major dihedral angles which depict the orientation of AM with respect to the phenyl ring *via* S atom, S18-C15-C12-C11, H16 -C15 -C12-C11, H19-S18-C15-C12 with the corresponding values 128.09°, 5.79°, 174.53° respectively, revealed the deviation of planarity by sulphur atom that leads to different conformations of the compound. The different conformations particularly arise due to the non-planarity of sulphur atom as the mercaptan bond can undergo free rotation.

The conformational behavior of the molecule provides useful information regarding drug actions. A detailed conformational theoretical analysis has been carried out in order to understand the conformational properties of the molecules. The presence of double bond on the AM results in the generation of cis and trans isomers. The trans isomer was predicted to be more stable than the cis form as predicted by the B3LYP/6-311G++(d,p) calculations. The internal rotation about the SH bond results in the conformational possibilities. The geometries of the three-possible configurations with their relative stabilities as determined from the excess Gibbs free energies calculated at same level of computation for aryl AM **1a** are displayed in Figure 2.

The relative stability of sub-conformations is not affected by different orientations of phenyl rings in the main configuration (maximum: 0.25 kcal/mol) [44]. Thus the order of decreasing stability of conformers in compound **1a** is i (0.0 kcal/mol) >ii (0.0025 kcal/mol) >iii (11.5137 kcal/mol).

The first conformation is the most stable form as the mercaptansulphur is eclipsed with hydrogens and methyl. For propionaldehyde the carbonyl oxygen is eclipsed with hydrogens and methyl and it has been shown by ^{1}HNMR spectra that such types are the preferred conformers in order to minimize the steric effect [45]. The conformational free energy of compound **1a** is approximately 11.5 kcal/mol in favor of the conformer **i** in which the mercaptansulphur is nearly eclipsed with methyl group. Similarly, for the compounds **1d**, **1e**, **1f**, and **1g** the lowest energy conformer as determined from the lowest Gibbs free energy values (Table 5) was found to be the one in which sulphur atom was eclipsing with methyl group (Figure 3). However, for the compounds **1b** and **1c** the lowest energy conformation had mercaptanhydrogen eclipsed with methyl group and such conformations are not present in detectable amount [46]. Thus the conformational results indicated that the lowest energy conformations for the compounds **1a, 1d, 1e, 1f and 1g** were more stable than for the compounds **1b** and **1c**. These lowest energy conformers have been used for the rest of the studies.

3.4. Frontier molecular orbitals

The calculated electronic properties are listed in Table 6. The compound **1a** has the lowest frontier orbital gap pertaining to its higher chemical reactivity (Figure 4). The negative chemical potential values for compounds **1(a-g)** indicate non-spontaneous decomposition which is a prerequisite of this study. The global hardness (η) depicts the resistance towards electron cloud deformation under perturbation observed in a chemical process [47,49].

Similarly, on the basis of frontier orbital gap, chemical potential and global hardness the compounds **1d, 1e, 1f** and **1g** had lesser frontier orbital gap and negative chemical potential compared to compounds **1b** and **1c** implying that compounds **1b** and **1c** are less reactive as compared to other compounds. For the compounds **1d, 1e, 1f** and **1g** the HOMO of sigma nature is localized over the sulphur atom while in LUMO the electron density is delocalized over the phenyl ring implying electron density transfer from the sulphur atom to the phenyl ring (Figure 5). This study provides an insight into the binding interactions which could occur majorly *via* the sulphur atom.

3.5. NBO analysis

The second order perturbation stabilization energy values E(2) (given in Table7) revealed significant interactions between Lewis and non-Lewis NBO orbitals for the compound **1a**. The transfer of electron density from oxygen atom lone pair (O22) in antibonding orbitals p(N20-O22) resulted in strong interaction with high stabilization energy 197.72 kcal/mol. Other important interactions include overlap of bonding p(C3-C4) with antibonding orbitals p(C11-C12), p(C5-C6) and p(C1 -C2) with corresponding stabilization energies 38.85, 25 and 20.51 kcal/mol respectively, bonding p(C5-C6) with antibonding orbitals p(C1-C2) and p(C3-C4) with corresponding stabilization energies 21.67 and 20.41 kcal/mol respectively, and bonding p(C1-C2) with antibonding orbitals p(C3-C4) and p(C5-C6) with stabilization energies 20.32 and 21.63 respectively. These interactions result in pronounced decrease in C3/C4, C5/C6 and C1/C2 orbital's occupancy (0.36548, 1.6525 and 1.67642 respectively). It also indicates a possibility of hyperconjugation within the phenyl ring and between the ring and allyl carbons. The lone pair interactions include overlap of lone pair (LP2) of oxygen atom (O21) to antibonding orbitals p*(N20-O22) with stabilization energy 15.94 kcal/mol. Similarly, the interaction of lone pair (LP2) of oxygen atom (O21) with p(C6-N20) has stabilization energy of 14.39 kcal/mol.

The NBO analysis predicts the stability of molecules arising from hyperconjugative interactions and charge delocalization. The results clearly show that electron density in anti-bonding orbitals and second order delocalization energies confirm the occurrence of inter-molecular charge transfer within the molecules [50].

These interactions indicate that the addition of electron withdrawing substituent to aromatic ring results in further molecular stabilization of the compound. Similarly, hyperconjugative interactions within the phenyl ring and between the ring and allyl carbons were seen for other compounds along with other interactions resulting in stabilization of the compounds **1(b-g)**.

3.6. Molecular docking

The overlapping of docked compounds **1(a-g)** with AM based 3D HDAC8 and HDAC3 binding model is depicted in Figure 6.

The conserved interacting amino acid residues were Tyr 306, His 180, Asp 267, Phe 152, Asp 178, His 142 and His 143. Docking investigations revealed the formation of metal coordinate bond between S and Zn at a distance of 2.348 Å, 2.358 Å and 2.362 Å for compounds **1a**, **1f** and **1g**,

respectively. The value for reference AM was 2.56 Å which indicates better binding affinity of compounds **1a**, **1f** and **1g** (Figure 7).

The glide score, gibbs energy values and Zn-S bond distances for the compounds are listed in Table 8.

The hydrophobic interactions were seen with residues Trp 141, Tyr 306, Met 274, Phe 208 and Phe 152 for all the compounds **1(a-g)** (Figure 8).

Polar interactions were observed with residues His 180 and His 142. There is preponderance of hydrophobic interactions on the linker chain which indicates that binding majorly takes place in the hydrophobic pocket of the receptor (Figure 9). It is well known through various published works and our own experiences that both hydrophobic as well as hydrogen binding interactions play pivotal role in complexation of ligands with proteins [45, 46, 47].

It has been reported that the benzyl mercaptan molecule bulkier than AM inhibited HDAC8 better than Hela nuclear extracts primarily containing HDAC3 indicating specific HDAC8 inhibition [29]. Watson *et al.* [48] predicted that the binding site of ligand in HDAC3 is far away from Zn atom a possible reason for selective binding to HDAC8. In the present study the designed aryl AM compounds bearing electron withdrawing groups 1(a-g)were docked with HDAC3 also. Figure 6 (II) depicts docked aryl AM compounds 1(a-g) with HDAC3.

The docking scores and Gibbs energy values were found to be good and comparable to the values as obtained for HDAC8 (Table 8). The non-covalent interactions like hydrophobic and Vander Waal interactions dominated the binding site. The results clearly state that these new designed aryl AM compounds bearing electron withdrawing substituents show general HDACI action and could be modified accordingly to treat multiple diseases.

4. Conclusion

A comprehensive *in silico* investigation of designed aryl AM compounds **1(a-g)** bearing electron withdrawing substituents was done. The most stable conformation calculated at DFT B3LYP/6-311G++(d,p) level of computation had methyl carbon eclipsed with mercaptansulphur. The structural parameters determined the planarity of the compounds except for sulphur atom which lies slightly above the plane. The electronic properties suggested high chemical reactivity. The NBO results indicated hyperconjugation within the phenyl ring and the ring with allyl carbons. The drug likeliness was confirmed *via*ADME. Docking data suggested the importance of hydrophobic interactions and metal coordination between the ligands **1(a-g)** and receptor. It supports the fact that substitution of aryl AM moiety with electron withdrawing substituents makes aryl AM better general HDACIs. Thus these potential HDACIs candidates could further help in design, development and screening of new pharmacaphores which could be modified for diversified pharmacological actions.

Declarations

Author contribution statement

Himanshu Ojha, Mallika Pathak, Paban K Agrawala: Conceived and designed the experiments; Analyzed and interpreted the data; Wrote the paper.

Sugandha Singhal: Conceived and designed the experiments; Performed the experiments; Analyzed and interpreted the data; Wrote the paper.

Funding statement

This research did not receive any specific grant from funding agencies in the public, commercial, or not-for-profit sectors.

Competing interest statement

The authors declare no conflict of interest.

Additional information

No additional information is available for this paper.

Acknowledgements

All authors are grateful to Director, INMAS for supporting this research work. All authors are grateful to Professor (Dr.) Rita Kakkar, Department of Chemistry, University of Delhi for providing her kind mentorship during the study.

References

[1] J.E. Bolden, M.J. Peart, R.W. Johnstone, Anticancer activities of histone deacetylase inhibitors, Nat. Rev. Drug Discov. 5 (2006) 769–784.
[2] L. Peng, E. Seto, Deacetylation of nonhistone proteins by HDACs and the implications in. cancer, Handb. Exp. Pharmacol. 206 (2011) 39–56.
[3] A.J. deRuijter, A.H. van Gennip, H.N. Caron, et al., Histone deacetylases (HDACs): characterization of the classical HDAC family, Biochem. J. 370 (2003) 737–749.
[4] G. Blander, L. Guarente, The Sir2 family of protein deacetylases, Annu. Rev. Biochem. 73 (2004) 417–435.
[5] S.G. Gray, T.J. Ekstrom, The human histone deacetylase family, Exp. Cell Res. 262 (2001) 75–83.
[6] J.R. Somoza, R.J. Skene, B.A. Katz, et al., Structural snapshots of human HDAC8 provide insights into the class I histone deacetylases, Structure 12 (2004) 1325–1334.
[7] E. Hu, Z. Chen, T. Fredrickson, et al., Cloning and characterization of a novel human class I histone deacetylase that functions as a transcription repressor, J. Biol. Chem. 275 (2000) 15254–15264.
[8] I. Van den Wyngaert, W. de Vries, A. Kremer, et al., Cloning and characterization of human histone deacetylase 8, FEBS Lett. 478 (2000) 77–83.
[9] J.J. Buggy, M.L. Sideris, P. Mak, et al., Cloning and characterization of a novel human histone deacetylase, HDAC8,Biochem. J. 350 (2000) 199–205.
[10] J. Li, J. Wang, J. Wang, et al., Both corepressor proteins SMRT and N-CoR exist in large protein complexes containing HDAC3, EMBO J. 19 (2000) 4342–4350.
[11] J. Zhang, M. Kalkum, B.T. Chait, et al., The N-CoR-HDAC3 nuclear receptor corepressor complex inhibits the JNK pathway through the integral subunit GPS2, Mol. Cell. 9 (2002) 611–623.
[12] Y.D. Wen, V. Perissi, L.M. Staszewski, et al., The histone deacetylase-3 complex contains nuclear receptor corepressors, Proc. Natl. Acad. Sci. U.S.A. 97 (2000) 7202–7207.
[13] M.G. Guenther, W.S. Lane, W. Fischle, et al., A core SMRT corepressor complex containing HDAC3 and TBL1, a WD40-repeat protein linked to deafness, Genes Dev. 14 (2000) 1048–1057.
[14] H.G. Yoon, D.W. Chan, Z.Q. Huang, et al., Purification and functional characterization of the human N-CoR complex: the roles of HDAC3, TBL1 and TBLR1, EMBO J. 22 (2003) 1336–1346.
[15] J. Oberoi, L. Fairall, P.J. Watson, et al., Structural basis for the assembly of the SMRT/NCoR core transcriptional repression machinery, Nat. Struct. Mol. Biol. 18 (2011) 177–184.
[16] M. Mottamal, S. Zheng, T.L. Huang, et al., Histone deacetylase inhibitors in clinical studies as templates for new anticancer agents, Molecules 20 (2015) 3898–3941.
[17] M. Dokmanovic, C. Clarke, P.A. Marks, Histone deacetylase inhibitors: overview and perspectives, Mol. Canc. Res. 5 (2007) 981–989.
[18] W.K. Rasheed, R.W. Johnstone, H.M. Prince, Histone deacetylase inhibitors in cancer therapy, Expet Opin. Invest. Drugs 16 (2007) 659–678.
[19] B.B. Aggarwal, S. Shishodia, Molecular targets of dietary agents for prevention and therapy of cancer, Biochem. Pharmacol. 71 (2006) 1397–1421.
[20] S.M. Meeran, A. Ahmed, T.O. Tollefsbol, Epigenetic targets of bioactive dietary components for cancer prevention and therapy, Clin. Epigenet. 1 (2010) 101–116.
[21] H.S. Park, G.Y. Kim, I.W. Choi, et al., Inhibition of matrix metalloproteinase activities and tightening of tight junctions by diallyl disulfide in AGS human gastric carcinoma cells, J. Food Sci. 76 (2011) 105–111.
[22] S. Yousuf, A. Ahmad, A. Khan, et al., Effect of diallyldisulphide on an antioxidant enzyme system in Candida species, Can. J. Microbiol. 56 (2010) 816–821.
[23] P.A. Marks, Discovery and development of SAHA as an anticancer agent, Oncogene 26 (2007) 1351–1356.
[24] A.H. Antosiewicz, A.A. Powolny, S.V. Singh, Molecular targets of cancer chemoprevention by garlic-derived organosulfides, Acta Pharmacol. Sin. 28 (2007) 1355–1364.
[25] L.Y. Sheen, C.C. Wu, C.K. Lii, et al., Metabolites of diallyl disulfide and diallyl sulfide in primary rat hepatocytes, Food Chem. Toxicol. 37 (1999) 1139–1146.

[26] M.A. Lea, M. Rasheed, V.M. Randolph, et al., Induction of histone acetylation and inhibition of growth of mouse erythroleukemia cells by S-allylmercaptocysteine, Nutr. Canc. 43 (2002) 90–102.
[27] N. Druesne, A. Pagniez, C. Mayeur, et al., Diallyl disulfide (DADS) increases histone acetylation and p21(waf1/cip1) expression in human colon tumor cell lines, Carcinogenesis 25 (2004) 1227–1236.
[28] T. Suzuki, A. Kouketsu, A. Matsuura, et al., Thiol-based SAHA analogues as potent histone deacetylase inhibitors, Bioorg. Med. Chem. Lett 14 (2004) 3313–3317.
[29] H. Nian, B. Delage, J.T. Pinto, et al., Allylmercaptan, a garlic-derived organosulfur compound, inhibits histone deacetylase and enhances Sp3 binding on the P21WAF1 promoter, Carcinogenesis 29 (2008) 1816–1824.
[30] S.K. Rai, M. Sharma, M. Tiwari, Synthesis, DNA binding, and cytotoxic evaluation of new analogs of Diallyldisulphide, an active principle of garlic, Bioorg. Med. Chem. 16 (2008) 7302–7310.
[31] C.A. Lipinski, F. Lombardo, B.W. Dominy, et al., Experimental and computational approaches to estimate solubility and permeability in drug discovery and development settings, Adv. Drug Deliv. Rev. 23 (1997) 3–25.
[32] Bioinformatics, Molecular Design Research Center, Seul, South Corea, PreADMET program, Available from: http://preadmet.bmdrc.org, 2004.
[33] L.C. Allen, Bibliography and theses, Int. J. Quant. Chem. 95 (2003) 663–677.
[34] R. Dennington, T. Keith, J. Millam, GaussView, Version 5, in: Semichem Inc., Shawnee Mission, KS, 2009.
[35] M.J. Frisch, G.W. Trucks, H.B. Schlegel, et al., Gaussian 09, Revision D.01, Gaussian, Inc., Wallingford CT, 2009.
[36] R. Al-Wabli, D. Manimaran, L. John, et al., Spectroscopic investigations, DFT calculations, and molecular docking studies of the anticonvulsant (2E)-2-[3-(1H-Imidazol-1-yl)-1-phenylpropylidene]-N-(4methylphenyl)hydrazinecarboxamide, J. Spectroscopy (2016).
[37] Y.S. Mary, K. Raju, C.Y. Panicker, et al., Molecular conformational analysis, vibrational spectra, NBO analysis and first hyperpolarizability of (2E)-3-(3-chlorophenyl)prop-2-enoic anhydride based on density functional theory calculations, Spectrochim. Acta A. Mol. Biomol. Spectrosc. 131 (2014) 471–483.
[38] G. Gece, The use of quantum chemical methods in corrosion inhibitor studies, Corros. Sci. 50 (2008) 2981–2992.
[39] M.A. Lea, M. Rasheed, V.M. Randolph, et al., Induction of histone acetylation and inhibition of growth of mouse erythroleukemia cells by S-allylmercaptocysteine, Nutr. Canc. 43 (2002) 90–102.
[40] E.D. Glendening, C.R. Landis, F. Weinhold, Natural bond orbital methods, WIREs, Comput. Mol. Sci. 2 (2012) 1–42.
[41] M.S. Almutairi, A.M. Alanazi, E.S. Al-Abdullah, et al., FT-IR and FT-Raman spectroscopic signatures, vibrationalassignments, NBO, NLO analysis and molecular docking study of2-{[5-(adamantan-1-yl)-4-methyl-4H-1,2,4-triazol-3-yl]sulfanyl}-N,N-dimethylethanamine,Spectrochim, Acta A Mol. Biomol. Spectrosc. 140 (2015) 1–14.
[42] R.A. Friesner, R.B. Murphy, M.P. Repasky, et al., Extra precision glide: docking and scoring incorporating a model of hydrophobic enclosure for protein-ligand complexes, J. Med. Chem. 49 (2006) 6177–6196.
[43] H. Ojha, K. Mishra, M.I. Hassan, et al., Spectroscopic and isothermal titration calorimetry studies of binding interaction of ferulic acid with bovine serum albumin, Thermochim. Acta 548 (2012) 56–64.
[44] P.D. Ross, S. Subramanian, Thermodynamics of protein association reactions: forces contributing to stability, Biochemistry 20 (1981) 3096–3102.
[45] G.J. Karabatsos, D.J. Fenoglio, Rotational isomerism about sp2-sp3 carbon-carbon single bonds, in: E.L. Eliel, N.L. Allinger (Eds.), Topics in Stereochemistry, John Wiley & Sons, Inc., Hoboken, NJ, USA, 1970, pp. 167–203.
[46] P.D. Ross, S. Subramanian, Thermodynamics of protein association reactions: forces contributing to stability, Biochemistry 20 (1981) 3096–3102.
[47] H.V. Movahed, M.R. Saberi, J. Chamani, Comparison of binding interactions ofLomefloxacin to serum albumin and serum transferrin by resonance light scattering and fluorescence quenching method, J. Biomol. Struct. Dyn. 28 (2011) 483–502.
[48] P.J. Watson, L. Fairall, G.M. Santos, et al., Structure of HDAC3 bound to co-repressor and inositol tetraphosphate, Nature 481 (2012) 335–340.
[49] L. Khanna, S. Singhal, S.C. Jain, et al., Spiro-indole-coumarin hybrids: synthesis, ADME, DFT, NBO studies and in silico screening through molecular docking on DNA G-Quadruplex, Chem. Sel. 5 (2020) 3420–3433.
[50] S. Singhal, P. Khanna, L. Khanna, Synthesis, DFT studies, molecular docking, antimicrobial screening and UV flourescence studies on ct-DNA for novel Schiff bases of 2-(1-aminobenzyl)benzimidazole, Heliyon 5 (2019) e02596.